Korean J. Chem. Eng., 36(12), 2104-2109 (2019)
DOI: 10.1007/s11814-019-0396-6

pISSN: 0256-1115
eISSN: 1975-7220

Facile fabrication and photocatalytic activity of Ag/AgI/rGO films

Sooyeon Jang*,‡, Sung Min Lee*,‡, Jin Seon You*, Hyung-Jun Koo,†, and Suk Tai Chang*,†**

*School of Chemical Engineering and Materials Science, Chung-Ang University, Seoul 06974, Korea
**Department of Chemical and Biomolecular Engineering, Seoul National University of Science and Technology, Seoul 01811, Korea
(*Received 25 May 2019 • accepted 26 September 2019*)

Abstract−The composite material, Ag/AgX/graphene (X=Br, Cl, I), is considered a promising photocatalyst for photocatalytic degradation of organic pollutants. Its photocatalytic activity is superior to that of the conventional TiO_2 photocatalyst; the enhanced photocatalytic activity is attributed to its effective charge separation ability and wide visible light absorption. However, the Ag/AgX/graphene composite is often prepared in the powder form, limiting its widespread application. In addition, the simple fabrication of Ag/AgX/graphene composite films is highly challenging. In this study, a simple solution-based process based on meniscus-dragging deposition is demonstrated for the fabrication of Ag/AgI/rGO composite films. Uniform catalyst films with reasonable photocatalytic activities can be easily fabricated by using this microliter-scale solution process.

Keywords: Photocatalyst, Solution Process, Graphene, Silver Nanowire, Silver Halide

INTRODUCTION

Considerable efforts have been devoted to the development of photocatalysts for the decomposition of organic pollutants into water and carbon dioxide, applicable in various fields such as water purification, antibacteria, deodorization, and decontamination [1-5]. Accordingly, titanium dioxide (TiO_2) has been widely investigated because of its versatility and processability, resulting from its nontoxicity and stability. However, it has the following limitations: (1) absorption of only ultraviolet (UV) light because of its wide band gap energy (3.2 eV), and (2) poor quantum yield because of the rapid recombination of photogenerated electrons and holes. Thus, a more efficient and effective visible light photocatalyst is required [6-9].

To develop visible-light-sensitive photocatalysts, noble metal nanoparticles, such as Au, Ag, and Pt, have been widely explored because of their strong visible light absorption, resulting from surface plasmon resonance (SPR) [10-12]. Particularly, Ag/AgX (X=Cl, Br, I) composites have received substantial attention as promising candidates because of their excellent photocatalytic activities under visible light irradiation [13-15], which is attributed to the synergistic effect of SPR of Ag nanoparticles and light-harvesting ability of AgX [16,17]. For example, Wang et al. prepared a plasmonic photocatalyst Ag@AgX (Br, I) with high photocatalytic activity for methyl orange (MO) decomposition under visible light irradiation by ion-exchange between Ag_2MoO_4 and HBr [18].

Graphene and reduced graphene oxide (rGO) have been applied as electron-acceptor layers, resulting in effective separation of photogenerated electron-hole pairs [19-22]. Accordingly, these carbon-based nanomaterials have been used to improve the photocatalytic efficiencies of Ag/AgX photocatalysts. For instance, Luo et al. synthesized a Ag/AgCl/rGO heterostructure photocatalyst by a hydrothermal technique; the photocatalyst exhibited a significantly higher photocatalytic activity than Ag/AgCl (without rGO) [23].

Photocatalysts are generally fabricated in the powder form; therefore, an additional separation process is required after the photocatalytic reaction, leading to increased processing cost. Nonetheless, the complete removal of nanosized catalyst powders from a mixture of catalyst and effluent solution after the photocatalytic reaction is highly challenging. A strategy to overcome this issue is to immobilize photocatalysts in the form of films or to embed them into matrices [24-26]. Ghosh et al. reported Ag/AgCl nanoparticles with core@shell structures embedded in an agarose matrix for organic contaminant degradation [27]. The Ag/AgCl nanoparticles were immobilized in the agarose matrix, and, therefore, could be recycled for repetitive decomposition of organic pollutants. Recently, Han et al. fabricated a Ag/AgCl micro-membrane at the air-liquid interface [24]. This photocatalyst in the membrane form effectively degraded MO and exhibited good reproducibility for several cycles of the photocatalytic test. However, the scalable and cost-effective fabrication of Ag/AgX/graphene photocatalysts is challenging.

In this study, we demonstrate a simple and scalable method involving meniscus-dragging deposition (MDD) and chemical reduction for the fabrication of Ag/AgI/rGO photocatalytic films [28-31]. First, uniform liquid thin films containing networks of Ag nanowires (AgNWs) on glass slides were prepared by the MDD method, resulting in uniformly networked AgNWs film after solvent dried. Then, GO was coated on the AgNWs by MDD, followed by treatment with HI vapor to reduce GO and form the Ag/AgI complex. During the HI treatment, Ag/AgI particles floated on the surface of the rGO films because the surface energy of the glass substrate was signifi-

†To whom correspondence should be addressed.
E-mail: stchang@cau.ac.kr, hjkoo@seoultech.ac.kr
‡These authors contributed equally to this work.

cantly higher than that of rGO. The elemental compositions, crystal structures, and photo responses of the prepared Ag/AgI/rGO composite films were determined by scanning electron microscopy (SEM), X-ray diffraction (XRD), and UV-visible (UV-vis) spectroscopy, respectively. Moreover, the photocatalytic activity of the Ag/AgI/rGO heterogeneous films toward the degradation of MO in water was evaluated.

EXPERIMENTAL

1. Fabrication of Ag/AgI/rGO Films

Heterogeneous Ag/AgI/rGO films were prepared by a two-step process involving (1) MDD and (2) reduction. First, the glass deposition plate and substrates (25×75 mm with plain ends, Fisher Scientific) were piranha-cleaned ($H_2O_2 : H_2SO_4$=1 : 1) for 30 min to increase their hydrophilicity and rinsed with deionized (DI) water. A suspension of 0.5 wt% AgNWs in isopropanol (IPA) purchased from Sigma Aldrich (Product No. 739448) was used as the Ag source; the average diameter and length of the AgNWs was 115 nm and 20-50 μm, respectively. Typically, 20 μl of the AgNW solution was injected between two glass slides, which were in contact with each other at an angle of 30°, and the deposition plate was moved back and forth using a motorized stage (AL1-1515-3S, Micro Motion Technology, Valley Center, USA) at constant speed of 20 mm s^{-1}. In the MDD process, the deposition number (DN) is defined as the number of back and forth movements in one cycle, and the number of coatings (NC) is defined as the number of repeating cycles involving solution injection, back and forth motion, and drying. For Ag NW deposition, DN and NC were set as 3 and 12, respectively. After deposition, the AgNW films were annealed on a hot plate at 250 °C for 20 min to remove the polyvinylpyrrolidone (PVP) layer on the AgNW surface. Then, GO dispersion solution (3.325 mg ml^{-1}; SKU-HCGO-W-175, Graphene Supermarket) was coated by the same process (NC=1 and DN=20) using 20 μl for one cycle. Next, the resultant AgNWs/GO films were reacted with acetic acid/HI mixture (5 : 2 volume ratio) vapor at 80 °C for 30-240 min. Finally, the obtained Ag/AgI/rGO heterogeneous photocatalyst films were gently rinsed with DI water and ethanol solution to remove the remaining HI.

2. Evaluation of Photocatalytic Activities of Ag/AgI/rGO Films

The photocatalytic activity of the prepared Ag/AgI/rGO films toward MO degradation under visible light irradiation was investigated. A 150 W halogen lamp (FOK-100W, Fiber Optic Korea) with a 420 nm short wave cut-off filter (PSI Trading Co., Ltd.) was used as the visible light source. The average light intensity falling on the film surfaces was approximately 0.015 mW cm^{-2}. The photocatalytic test bath was prepared using an aqueous suspension of MO (0.02 g l^{-1} in 30 ml of DI water). For the measurements, the Ag/AgI/rGO films were immersed in the test bath. Typically, before light irradiation, the test bath with the film was kept in the dark-room for 1 h to attain the adsorption-desorption equilibrium. Subsequently, the MO concentration was determined by UV-vis-near infrared (NIR) spectrophotometry during the photocatalytic activity test (Fig. S2).

3. Characterization

The field-emission SEM (FE-SEM) images, energy-dispersive X-ray spectroscopy (EDS) maps, and overall atomic composition data of the prepared Ag/AgI/rGO films were obtained using a Carl Zeiss SIGMA instrument. In addition, the films were characterized by UV-vis-NIR spectrophotometry (V-670, Jasco) and XRD (D8

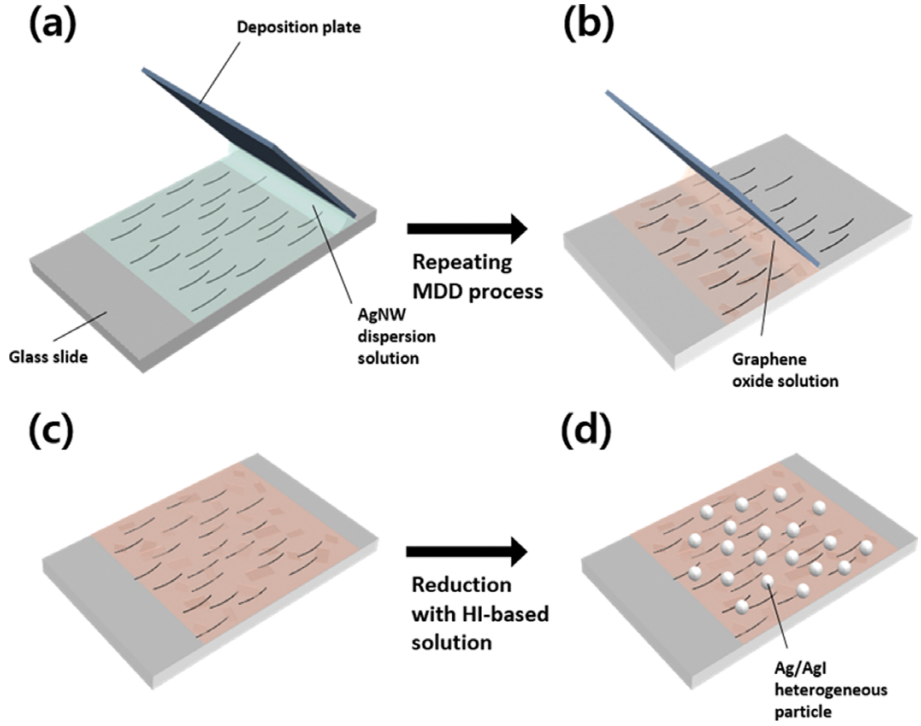

Fig. 1. Schematic of Ag/AgI/rGO film fabrication.

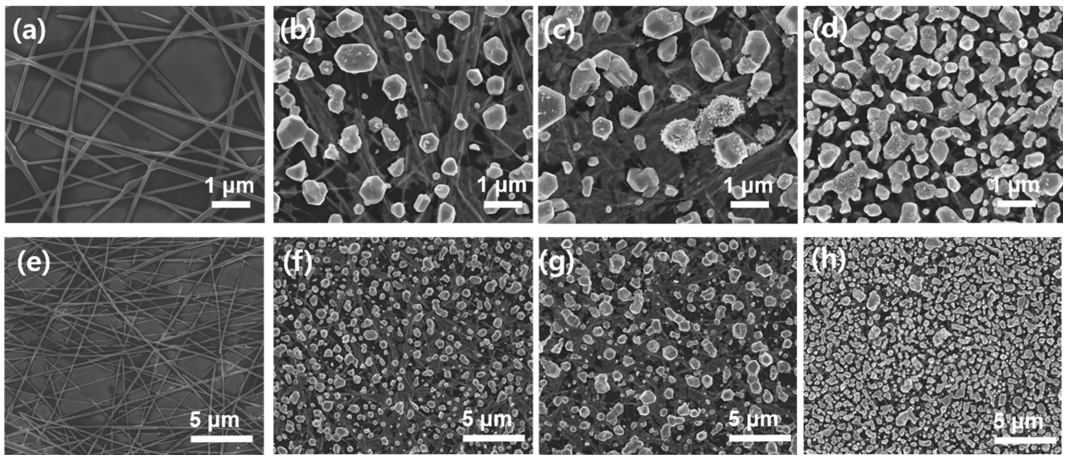

Fig. 2. FE-SEM images of (a), (e) Ag/GO film and Ag/AgI/rGO films with different reduction time. (b), (f) 30 min, (c), (g) 120 min, (d), (h) 240 min.

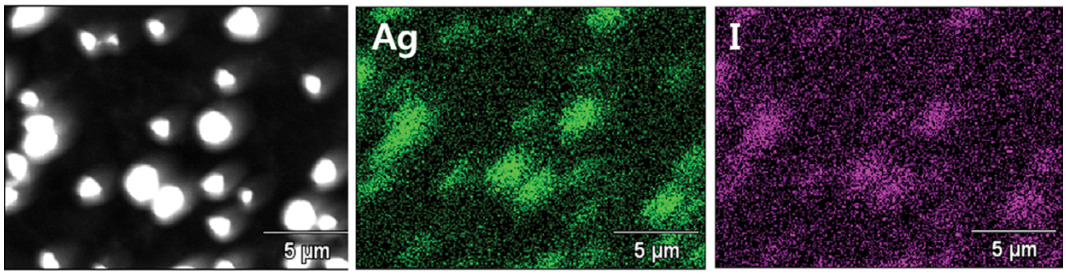

Fig. 3. SEM and corresponding EDS mapping images of the Ag/AgI/rGO film obtained by HI reduction for 120 min.

Advance, Bruker AXS). Surface morphology of Ag/AgI/rGO films was investigated by atomic force microscopy (NX-10 Complete, Park systems). The surface atomic composition was determined by X-ray photoelectron spectroscopy (XPS; K-Alpha+, Thermo Fisher).

RESULTS AND DISCUSSION

Ag/AgI/rGO films were prepared by a two-step method: deposition of AgNWs and GO flakes by the MDD method, followed by chemical reduction of the prepared Ag/GO film with HI vapor (Fig. 1). First, the AgNW/IPA suspension was injected between the deposition plate and the glass substrate, and because of capillary force, a meniscus was formed. Then, the AgNW suspension was dragged onto the substrate by moving the deposition plate back and forth, thereby forming a liquid thin film containing AgNWs. Subsequently, IPA was removed from the film to obtain a network of AgNWs aligned in the coating direction because of shear stress (Fig. 1(a)) [32]. The resultant film was annealed to remove the PVP capping layer on the AgNWs. Next, GO was deposited on the AgNWs by MDD (Fig. 1(b)). Then, the Ag/GO film was reacted with HI/acetic acid vapor (2 : 5 volume ratio) for a specific time (30, 120, or 240 min) to obtain a Ag/AgI/rGO film (Fig. 1(c) and 1(d)). The FE-SEM images in Fig. 2 reveal the morphology of the Ag/AgI/rGO heterostructure films. Ag/AgI particles can be observed on the surface of rGO. During reaction with HI vapor, Ag/AgI heterogeneous particles translocate with the rGO sheets, which cover the glass slide surface, to relieve the surface energy; the surface energy of glass (105 mJ m^{-2}) is much higher than that of rGO (28.2 mJ m^{-2}) [33]. As can be seen in Fig. 2(a)-(d), the Ag/AgI particle size decreases with increasing reaction time. In addition, the surface density of the particles increases with the reduction time. The morphology of Ag/AgI/rGO composite films was investigated using AFM and summarized in Fig. S1. The overall thickness of Ag/AgI/rGO composite film is 412±45 nm and the particle density increases as the reaction time with HI increases, corresponding to the FE-SEM image in Fig. 2.

To confirm the formation of Ag/AgI heteroparticles on rGO, the elemental composition of the prepared Ag/AgI/rGO composite films was determined by EDS (Fig. 3). The results show that the particles on the rGO surface are composed of Ag and I, indicating the formation of Ag/AgI complex particles by reduction of AgNWs with HI vapor. The Ag and I ratios of the particles for different

Table 1. Summary of elemental analysis results of Ag/AgI/rGO films obtained by HI reduction for different times

Reduction time (min)	Atomic content (at%)	
	Ag	I
30	70.90	29.10
120	70.26	29.74
240	61.56	38.44

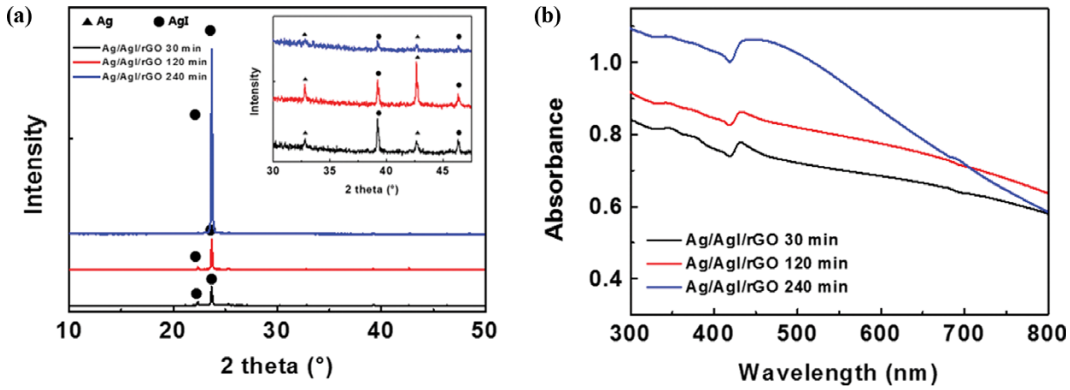

Fig. 4. (a) XRD patterns of Ag/AgI/rGO films obtained by HI reduction for different times and (b) UV-vis absorption spectra.

reduction times are summarized in Table 1. As the reduction time increases from 30 min to 240 min, the atomic content of I increases from 29.10% to 38.44%. Therefore, the amount of AgI in the Ag/AgI heterogeneous particles on rGO increases with the reduction time.

To further confirm the reduction of GO into rGO and conversion of Ag into Ag/AgI heteroparticles after reaction with HI vapor, XRD was performed on the Ag/AgI/rGO films (Fig. 4(a)). The XRD patterns reveal the formation of both hexagonal β-AgI (22.3° and 23.6°; JCPDS No. 85-0801) and cubic γ-AgI (39.2° and 46.3°, No. 09-0399). The Ag-rich particles crystallized into γ-AgI, as previously reported [27]. As the reduction reaction progressed, the Ag phase in the Ag/AgI heterogeneous particles gradually transformed into the AgI phase. Thus, the relative intensity of the β-AgI peak increased and that of the γ-AgI peak decreased. Although the broad diffraction peak at 24° corresponding to rGO is observed, it is overshadowed by the AgI peak at the same position. Moreover, the GO diffraction peak at 11.07° cannot be observed for the samples obtained at higher reduction times, indicating the complete reduction of GO into rGO.

To investigate the effect of reduction time on the photoresponsive characteristics of the prepared Ag/AgI/rGO films, UV-vis absorption spectroscopy analysis was performed (Fig. 4(b)). Wide-range light absorption from 300 nm to 800 nm is observed for the samples, and the absorption at around 430 nm significantly increases as the reaction time with HI vapor increases from 30 min to 240 min. Because the characteristic absorption of AgNWs occurs at around 345 nm and that of AgI occurs in the range from 300 nm to 500 nm, the wide-range absorption observed for the Ag/AgI/rGO films (300 nm to 800 nm) is attributed to electromagnetic coupling between the Ag and AgI particles [34]. With increasing reduction time, the number density of the Ag/AgI particles increases (as confirmed by the FE-SEM images in Fig. 2), resulting in an enhancement of electromagnetic coupling and SPR of the Ag/AgI particles. Therefore, among the Ag/AgI/rGO films, the one obtained by reduction for 240 min absorbs the largest amount of visible light [35-37].

The photocatalytic activity of the Ag/AgI/rGO films obtained by reduction for different times toward MO photocatalytic decomposition was evaluated. The reaction kinetics of heterogeneous photocatalysts can be described by using Langmuir-Hinshelwood (LH) models [38]. The typical reaction rate equation is given below:

$$-r_i = -\frac{dC_i}{dt} = \frac{k_{i,L-H}K_iC_i}{1+K_iC_i} \quad (1)$$

where $k_{i,L-H}$, K_i, and C_i are the apparent rate constant, sorption rate constant, and reactant concentration, respectively. At a low reactant concentration, Eq. (1) can be simplified to a first-order equation:

$$-\frac{dC}{dt} = kC \quad (2)$$

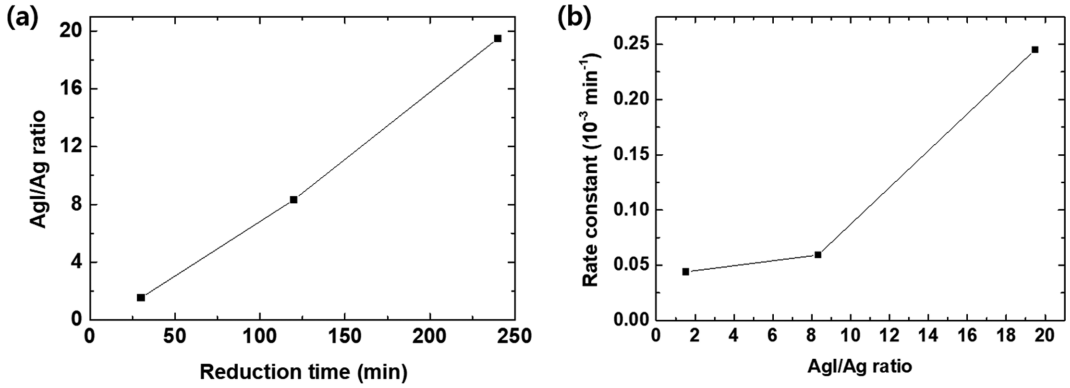

Fig. 5. (a) AgI/Ag ratio of Ag/AgI/rGO composite in the surface, determined by XPS. (b) Rate constant (k) of MO degradation by Ag/AgI/rGO films with different AgI/Ag ratio under visible light irradiation (λ>420 nm).

The reaction rate constant k (min^{-1}) can be obtained from the plot of C/C_0 versus time. The rate constant values for the Ag/AgI/rGO films were calculated according to this simplified model (Fig. 5). Among the Ag/AgI/rGO composite films, the one obtained after reduction for 240 min exhibits the highest photocatalytic activity with $k=0.25\times10^{-3}$ min^{-1}, which is about five times larger than that for the Ag/AgI/rGO film obtained after reduction for 30 min. To investigate the operation stability, the rate constant of the Ag/AgI/rGO composite films in the second reaction cycle was measured. The rate constant of the second cycle is $k=0.26\times10^{-3}$ min^{-1}, which is almost the same as that from the first cycle. It was also confirmed that the composite film was highly stable even under vigorous agitation, such as shaking or washing (Fig. S4). Note that the light intensity of the 150 W halogen lamp (0.015 mW cm^{-2}) used in this study is a hundred times lower than those of the light sources used in previous studies; therefore, we believe that by increasing the light intensity, higher photocatalytic reaction rates can be achieved [39-41]. The good photocatalytic activity of the Ag/AgI/rGO films is attributed to the efficient electron-hole pair separation by rGO. The provisional mechanism for photocatalytic decomposition by the Ag/AgI/rGO film is schematically shown in Fig. 6. Electron-hole pairs are generated on Ag by SPR upon visible light absorption and the excited electrons are transferred to the conduction band (CB) of AgI [23,42,43]. Then, the rGO, known as an effective electron acceptor, attracts the excited electrons from AgI, resulting in suppressing recombination of the photo-induced electron-hole pairs [23,44,45]. For comparison, we measured the photocatalytic activity of AgNW only, and Ag/AgI only films without rGO. None of the samples shows any measurable photocatalytic activity under the illumination condition of this study, which confirms the importance of rGO as an electron acceptor for high photocatalytic activity (Fig. S3). Subsequently, the excited electrons transferred to rGO reduce O_2 molecules to form superoxide anion radical, while the holes remaining on Ag oxidize water molecules to form hydroxyl radicals. Such highly reactive radicals formed by Ag/AgI/rGO composite decompose MO dye molecules. Thus, upon illumination of visible light, the Ag/AgI/rGO film photocatalytically decompose by forming reactive radicals, where rGO plays an important role in efficient electron-hole pair separation and the high photocatalytic activity of the composite film [44,46,47].

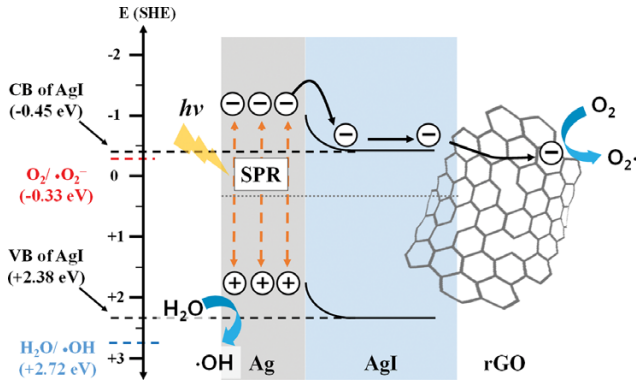

Fig. 6. Photocatalytic mechanism of radical formation and electron transfer in Ag/AgI/rGO composite SPR, C.B and V.B are surface plasmon resonance, conduction band and valence band, respectively.

CONCLUSION

Ag/AgI/rGO heterogeneous photocatalytic films were fabricated by a two-step process involving MDD and chemical reduction. The SEM, EDS, and XRD data for the films confirmed that HI treatment of the AgNW/GO films prepared by MDD led to Ag/AgI complexation and GO reduction. The as-obtained Ag/AgI/rGO films exhibited efficient photocatalytic degradation of the organic dye MO under visible light irradiation. The Ag/AgI/rGO film obtained after HI reduction for 240 min exhibited an MO decomposition rate 5.56 times higher than that of the film obtained after reduction for 30 min, because of enhanced SPR of the Ag nanostructures. The photocatalytic activity enhancement could be attributed to the effective separation of photogenerated charge carriers, facilitated by Ag/AgI/rGO bandgap matching. The Ag/AgI/rGO film fabrication method developed in this study is facile, scalable, and inexpensive. We believe that the prepared Ag/AgI/rGO films are efficient and recyclable photocatalytic platforms for water purification and decontamination.

ACKNOWLEDGEMENTS

This work was supported by the National Research Foundation of Korea (NRF) grant funded by the Korean government (No. 2019R1A2C1006413) and the Chung-Ang University Graduate Research Scholarship in 2018.

SUPPORTING INFORMATION

Additional information as noted in the text. This information is available via the Internet at http://www.springer.com/chemistry/journal/11814.

REFERENCES

1. S. W. Chook, C. H. Chia, S. Zakaria, M. K. Ayob, K. L. Chee, N. M. Huang, H. M. Neoh, H. N. Lim, R. Jamal and R. M. F. R. A. Rahman, *Nanoscale Res. Lett.*, **7**, 541 (2012).
2. V. Etacheri, G. Michlits, M. K. Seery, S. J. Hinder and S. C. Pillai, *ACS Appl. Mater. Interfaces*, **5**, 1663 (2013).
3. S. Gelover, P. Mondragón and A. Jiménez, *J. Photochem. Photobiol. A Chem.*, **165**, 241 (2004).
4. F. Motahari, M. R. Mozdianfard, F. Soofivand and M. Salavati-Niasari, *RSC Adv.*, **4**, 27654 (2014).
5. J. Peral, X. Domènech and D. F. Ollis, *J. Chem. Technol. Biotechnol.*, **70**, 117 (1997).
6. K. Hashimoto, H. Irie and A. Fujishima, *Japanese J. Appl. Physics*, **44**, 8269 (2005).
7. M. N. Chong, B. Jin, C. W. K. Chow and C. Saint, *Water Res.*, **44**, 2997 (2010).
8. M. Ni, M. K. H. Leung, D. Y. C. Leung and K. Sumathy, *Renew. Sustain. Energy Rev.*, **11**, 401 (2007).
9. X. Zhang, Y. L. Chen, R. S. Liu and D. P. Tsai, *Reports Prog. Phys.*,

76, 046401 (2013).
10. K. Drew, G. Girishkumar, K. Vinodgopal and P. V. Kamat, *J. Phys. Chem. B*, **109**, 11851 (2005).
11. Y. Wang, F. Wang and J. He, *Nanoscale*, **5**, 11291 (2013).
12. D. Chatterjee, V. R. Patnam, A. Sikdar, P. Joshi, R. Misra and N. N. Rao, *J. Hazard. Mater.*, **156**, 435 (2008).
13. X. Ma, Y. Dai, M. Guo and B. Huang, *ChemPhysChem*, **13**, 2304 (2012).
14. C. Zeng, B. Tian and J. Zhang, *J. Colloid Interface Sci.*, **405**, 17 (2013).
15. P. Wang, B. Huang, X. Zhang, X. Qin, Y. Dai, Z. Wang and Z. Lou, *ChemCatChem*, **3**, 360 (2011).
16. L. J. Sherry, S. H. Chang, G. C. Schatz, R. P. Van Duyne, B. J. Wiley and Y. N. Xia, *Nano Lett.*, **5**, 2034 (2005).
17. T. R. Jensen, M. D. Malinsky, C. L. Haynes and R. P. Van Duyne, *J. Phys. Chem. B*, **104**, 10549 (2000).
18. P. Wang, B. Huang, X. Zhang, X. Qin, H. Jin, Y. Dai, Z. Wang, J. Wei, J. Zhan, S. Wang, J. Wang and M. H. Whangbo, *Chem. Eur. J.*, **15**, 1821 (2009).
19. M. Zhu, P. Chen and M. Liu, *ACS Nano*, **5**, 4529 (2011).
20. G. Williams, B. Seger and P. V. Kamt, *ACS Nano*, **2**, 1487 (2008).
21. X. H. Meng, X. Shao, H. Y. Li, J. Yin, J. Wang, F. Z. Liu, X. H. Liu, M. Wang and H. L. Zhong, *Mater. Lett.*, **105**, 162 (2013).
22. Q. Xiang, J. Yu and M. Jaroniec, *Chem. Soc. Rev.*, **41**, 782 (2012).
23. G. Luo, X. Jiang, M. Li, Q. Shen, L. Zhang and H. Yu, *ACS Appl. Mater. Interfaces*, **5**, 2161 (2013).
24. L. Han, Z. Xu, P. Wang and S. Dong, *Chem. Commun.*, **49**, 4953 (2013).
25. Q. Xiang, J. Yu and M. Jaroniec, *Chem. Commun.*, **47**, 4532 (2011).
26. J. Zhou, Y. Cheng and J. Yu, *J. Photochem. Photobiol. A Chem.*, **223**, 82 (2011).
27. S. Ghosh, A. Saraswathi, S. S. Indi, S. L. Hoti and H. N. Vasan, *Langmuir*, **28**, 8550 (2012).
28. Y. U. Ko, S. R. Cho, K. S. Choi, Y. Park, S. T. Kim, N. H. Kim, S. Y. Kim and S. T. Chang, *J. Mater. Chem.*, **22**, 3606 (2012).
29. Y. Ko, N. H. Kim, N. R. Lee and S. T. Chang, *Carbon*, **77**, 964 (2014).
30. N. H. Kim, Y. Ko, S. R. Cho and S. T. Chang, *J. Nanosci. Nanotechnol.*, **14**, 3774 (2014).
31. Z. Yin, S. K. Song, D. J. You, Y. Ko, S. Cho, J. Yoo, S. Y. Park, Y. Piao, S. T. Chang and Y. S. Kim, *Small*, **11**, 4576 (2015).
32. Y. Ko, S. K. Song, N. H. Kim and S. T. Chang, *Langmuir*, **32**, 366 (2016).
33. N. H. Kim, B. J. Kim, Y. Ko, J. H. Cho and S. T. Chang, *Adv. Mater.*, **25**, 894 (2013).
34. Y. Liang, H. Wang, L. Liu, P. Wu, W. Cui, J. G. McEvoy and Z. Zhang, *J. Mater. Sci.*, **50**, 6935 (2015).
35. C. Noguez, *J. Phys. Chem. C*, **111**, 3606 (2007).
36. J. Ye, F. Wen, H. Sobhani, J. B. Lassiter, P. Van Dorpe, P. Nordlander and N. J. Halas, *Nano Lett.*, **12**, 1660 (2012).
37. H. Liang, H. Tian and R. L. McCreery, *Appl. Spectrosc.*, **61**, 613 (2007).
38. P. Zamostny and Z. Belohlav, *Appl. Catal. A Gen.*, **225**, 291 (2002).
39. M. N. Rashed and A. A. El-Amin, *Int. J. Phys. Sci.*, **2**, 73 (2007).
40. S. Tabata, H. Ohnishi, E. Yagasaki, M. Ippommatsu and K. Domen, *Catal. Lett.*, **28**, 417 (1994).
41. Y. Nosaka and A. Y. Nosaka, *J. Phys. Chem. C*, **122**, 28748 (2018).
42. M. Ren, J. Chen, P. Wang, J. Hou, J. Qian, C. Wang and Y. Ao, *J. Colloid Interface Sci.*, **532**, 190 (2018).
43. C. Hu, T. Peng, X. Hu, Y. Nie, X. Zhou, J. Qu and H. He, *J. Am. Chem. Soc.*, **132**, 857 (2010).
44. D. A. Reddy, S. Lee, J. Choi, S. Park, R. Ma, H. Yang and T. K. Kim, *Appl. Surf. Sci.*, **341**, 175 (2015).
45. R. Vinoth, P. Karthik, C. Muthamizhchelvan, B. Neppolian and M. Ashokkumar, *Phys. Chem. Chem. Phys.*, **18**, 5179 (2016).
46. F. Zheng, W. L. Xu, H. D. Jin, X. T. Hao and K. P. Ghiggino, *RSC Adv.*, **5**, 89515 (2015).
47. X. Zhang, Y. L. Chen, R. S. Liu and D. P. Tsai, *Rep. Prog. Phys.*, **76**, 046401 (2013).

Supporting Information

Facile fabrication and photocatalytic activity of Ag/AgI/rGO films

Sooyeon Jang[*,‡], Sung Min Lee[*,‡], Jin Seon You[*], Hyung-Jun Koo[,†], and Suk Tai Chang[*,†]**

*School of Chemical Engineering and Materials Science, Chung-Ang University, Seoul 06974, Korea
**Department of Chemical and Biomolecular Engineering, Seoul National University of Science and Technology, Seoul 01811, Korea
(*Received 25 May 2019 • accepted 26 September 2019*)

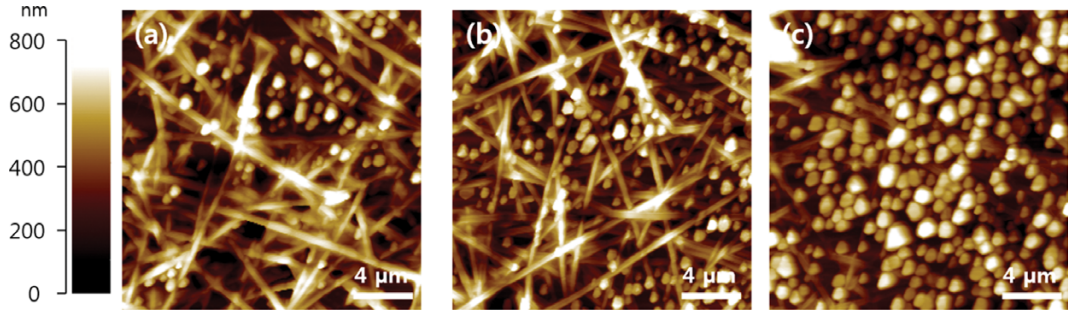

Fig. S1. AFM images of Ag/AgI/rGO composite film with reduction time of (a) 30 min, (b) 120 min, and (c) 240 min.

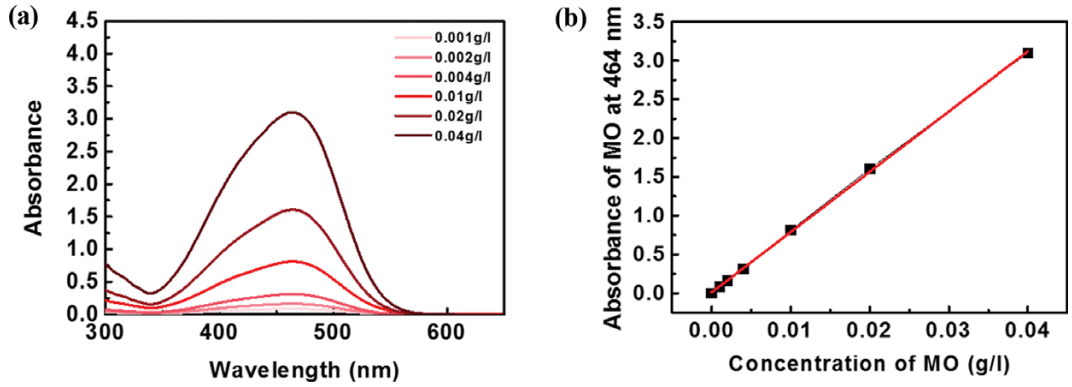

Fig. S2. (a) Variation in the absorbance of MO with concentration and (b) calibration curve for MO at ca. 464 nm.

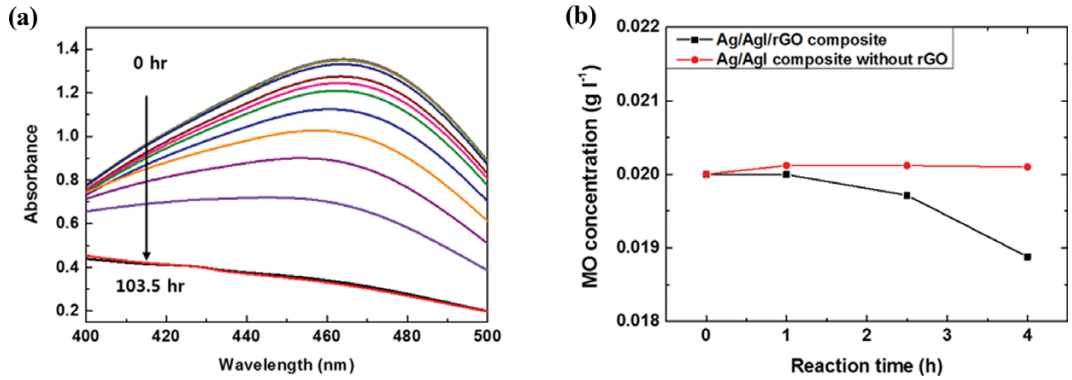

Fig. S3. (a) Change of UV/Vis spectrum of the aqueous solution in presence of Ag/AgI/rGO 240 min film under visible light irradiation (λ>420 nm). (b) Comparison of MO degradation between Ag/AgI/rGO composite and Ag/AgI composite without rGO.

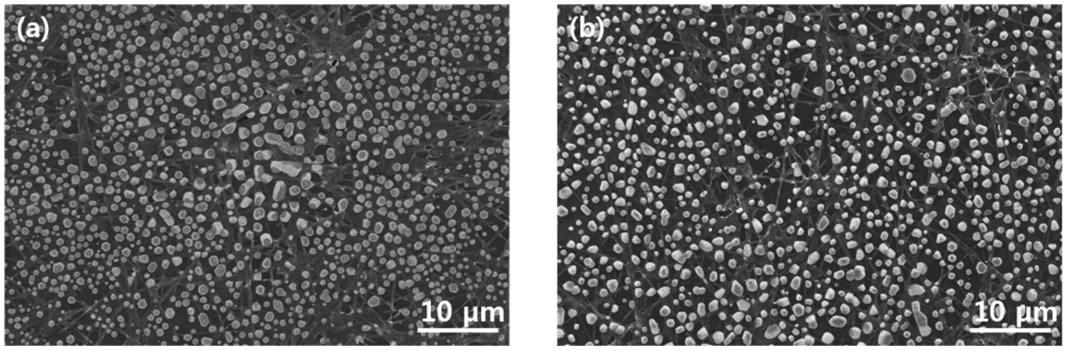

Fig. S4. FE-SEM image of Ag/AgI/rGO film (a) after recycling test and (b) after 30 min washed with D. I. water at 100 rpm on orbital shaker.